AN IMPROVED CEBECI-SMITH TURBULENCE MODEL FOR BOUNDARY-LAYER AND NAVIER-STOKES METHODS

Tuncer Cebeci
Professor and Chair, Aerospace Engineering Dept.
California State University, Long Beach, CA, USA

K.C. Chang
McDonnell Douglas Corporation, USA

Abstract

The accuracy of the turbulence models based on the algebraic eddy viscosity formulation of Cebeci and Smith (CS) is investigated for predicting the performance of airfoils at low Mach numbers for a wide range of angles of attack, including stall and post stall. The models include the Baldwin-Lomax model, the original CS model with length scale recommendations due to Stock and Haase and Johnson, the Johnson and King (JK) model, and a modified CS model due to the present authors. The calculated results obtained with interactive boundary-layer and Navier-Stokes methods indicate that all models considered give similar results at low to moderate angles of attack; at higher angles of attack, near stall and post stall, only the JK and modified CS models produce results which are in good agreement with data.

Introduction

Today, most Navier-Stokes methods employ the Baldwin-Lomax turbulence model,(1) which is a modified version of the Cebeci-Smith (CS) algebraic eddy-viscosity model developed for boundary-layer flows.(2) The main difference between the two models lies in the length scale used in the outer eddy viscosity. The Cebeci and Smith formulation uses the displacement thickness δ^* as the length scale; since δ^* is not well defined in the Navier-Stokes calculations due to the lack of precise definition of the boundary-layer thickness, Baldwin and Lomax use alternative expressions for the length scale. The studies conducted by Stock and Haase, (3) however, clearly demonstrate that the modified algebraic eddy-viscosity formulation of Baldwin and Lomax is not a true representation of the CS model, since their incorporation of the length scale in the outer eddy viscosity is not appropriate for flows with strong pressure gradient.

Studies conducted with Navier-Stokes methods using the Baldwin-Lomax model confirm the studies of Stock and Haase(3) and indicate a need for a better model. The Cebeci-Smith model, on the other hand, while satisfactory at low to moderate pressure gradient flows, requires improvements for strong pressure gradient flows that are typical to flows either approaching stall or post-stall.

The main weakness in the CS model is the parameter α used in the outer eddy-viscosity formula, which in the original formulation was taken as 0.0168. Experiments indicate, however, that in strong pressure gradient flows, the extent of the law of the wall region becomes smaller; to predict flows under such conditions, it is necessary to have a smaller value of α in the outer eddy-viscosity formula. The question is how to relate α to the flow properties so that the influence of adverse pressure gradient is included in the variation of α.

In this paper we discuss an improved CS model for boundary-layer and Navier-Stokes methods and present results obtained with this model as well as with other models based on the original CS model. In the following section we first present a brief description of the original CS model and its modified versions in order to adopt this model into Navier-Stokes methods. This section is followed by a discussion and review of the improvements proposed to the CS model, either for boundary-layer methods or Navier-Stokes methods. Calculated results obtained with the interactive boundary-layer method of Cebeci(4,5) as well as with the Navier-Stokes method of Swanson and Turkel(6) are presented in Results and Discussion Section.

Original CS Model And Its Modified Versions

The Cebeci-Smith model treats a turbulent boundary-layer as a composite layer with inner and outer regions. In the inner region of a smooth surface without mass transfer, the eddy viscosity $(\varepsilon_m)_i$ is written as

$$\left(\varepsilon_m\right)_i = \ell^2\left|\frac{\partial u}{\partial y}\right|\gamma_{tr}, \quad 0 \le y \le y_c \tag{1}$$

Here the mixing length ℓ is given by

$$\ell = \kappa y\left[1 - exp\left(-\frac{y}{A}\right)\right] \tag{2a}$$

where $\kappa = 0.40$ and A is a damping-length constant represented by

$$A = 26\,\nu\, u_\tau^{-1}, \quad u_\tau = \left(\frac{\tau}{\rho}\right)_{max}^{1/2},$$
$$\frac{\tau}{\rho} = \left(\nu + \varepsilon_m\right)\frac{\partial u}{\partial y} \tag{2b}$$

In Eq. (1) γ_{tr} is an intermittency factor which represents the streamwise region from the onset of transition to turbulent flow. It is given by

$$\gamma_{tr} = 1 - exp\left[-G\left(x - x_{tr}\right)\int_{x_{tr}}^{x}\frac{dx}{u_e}\right] \tag{3}$$

where x_{tr} is the location of the onset of transition; factor G has the dimensions of *velocity/(length)* and is evaluated at the transition location by

$$G = \frac{3}{C^2}\frac{u_e^3}{\nu^2}R_{x_{tr}}^{-1.34} \tag{4}$$

where the transition Reynolds number $R_{x_{tr}}$ is $\left(u_e x/\nu\right)_{tr}$ and C is a constant with a recommended value of 60.

In the outer region, the eddy viscosity is given by

$$\left(\varepsilon_m\right)_o = \alpha u_e \delta^* \gamma_{tr}\gamma, \quad y_c \le y \le \delta \tag{5}$$

Here γ is the intermittency factor for the outer region. With y_o defined as the y location where $u/u_e = 0.995$, it is given by

$$\gamma = \left[1 + 5.5\left(\frac{y}{y_o}\right)^6\right]^{-1} \tag{6}$$

based on Klebanoff's measurements on a flat plate flow. Continuity of the expressions for the eddy viscosities in the inner and outer regions, Eqs. (1) and (5), defines the boundaries of inner and outer regions. The parameter α, in Eq. (5) is equal to 0.0168.

Due to its simplicity and its good success in external boundary-layer flows, this model with modifications has also been used extensively in the solution of the Reynolds-averaged Navier-Stokes equations for turbulent flows. For the inner region, Baldwin and Lomax(1) use the expressions given by Eqs. (1) and (2). In the outer region, they use alternative expressions for the length scale δ^* of the form

$$\left(\varepsilon_m\right)_o = \alpha c_1 \gamma y_{max} F_{max} \tag{7a}$$

or

$$\left(\varepsilon_m\right)_o = \alpha c_1 \gamma c_2 u_{diff}^2 \frac{y_{max}}{F_{max}} \tag{7b}$$

with $c_1 = 1.6$ and $c_2 = 0.25$. The quantities F_{max} and y_{max} are determined from the function

$$F = y\left(\frac{\partial u}{\partial y}\right)\left[1 - e^{-y/A}\right] \tag{8}$$

with F_{max} corresponding to the maximum value of F that occurs in a velocity profile and y_{max} denoting the y-location of F_{max}. u_{diff} is the difference between maximum and minimum velocity in the profile

$$u_{diff} = u_{max} - u_{min} \tag{9}$$

where u_{min} is taken to be zero except in wakes.

In Navier-Stokes calculations, Baldwin and Lomax replace the absolute value of the velocity gradient $\partial u/\partial y$ in Eqs. (1) and (8) by the absolute value of the vorticity $|\omega|$,

$$|\omega| = \left|\frac{\partial u}{\partial y} - \frac{\partial v}{\partial x}\right| \tag{10a}$$

and the intermittency factor γ in Eq. (6) is written as

$$\gamma = \left[1 + 5.5\left(\frac{c_3 y}{y_{max}}\right)^6\right]^{-1} \tag{10b}$$

with $c_3 = 0.3$. The studies conducted by Stock and Haase[3] clearly demonstrate that the modified algebraic eddy viscosity formulation of Baldwin and Lomax is not a true representation of the CS model since their incorporation of the length scale in the outer eddy viscosity formula is not appropriate for flows with strong pressure gradients.

Stock and Haase proposed a length scale based on the properties of the mean velocity profile calculated by a Navier-Stokes method. They recommend computing the boundary-layer thickness δ from

$$\delta = 1.936\, y_{max} \qquad (11)$$

where y_{max} is the distance from the wall for which $y|\partial u/\partial y|$ or F in Eq. (8) has its maximum. With δ known, u_e in the outer eddy viscosity formula, Eq. (5), is the u at $y = \delta$, and γ is computed from Eq. (6) and not from Eq. (10b). The displacement thickness δ^* for attached flows is computed from its definition,

$$\delta^* = \int_o^{\delta} \left(1 - \frac{u}{u_e}\right) dy \qquad (12a)$$

and, for separated flows from

$$\delta^* = \int_{y_{u=0}}^{\delta} \left(1 - \frac{u}{u_e}\right) dy \qquad (12b)$$

either integrating the velocity profile from $y = 0$, or $y = y_{u=0}$, to δ, or using the Coles velocity profile. The results obtained with this modification to the length scale in the outer CS eddy viscosity formula improve the predictions of the CS model in Navier-Stokes methods as discussed in Stock and Haase. [3]

A proposal which led to Eq. (11) was also made by Johnson. [7] He recommended that the boundary-layer thickness δ is calculated from

$$\delta = 1.2 y_{1/2} \qquad (13)$$

where

$$y_{1/2} = y \quad \text{at} \quad \frac{F}{F_{max}} = 0.5 \qquad (14)$$

Improvements to the Original CS Model

Extensive studies, mostly employing boundary-layer equations, show that while many external turbulent flow problems can satisfactorily be calculated with the original Cebeci-Smith eddy-viscosity formulation, improvements are needed for flows which contain regions of strong pressure gradient and flow separation. One approach developed by Johnson and King[8] and Johnson and Coakley[9] is to adopt a nonequilibrium eddy-viscosity formulation ε_m in which the CS model serves as an equilibrium eddy viscosity $(\varepsilon_m)_{eq}$ distribution. An ordinary differential equation (ODE), derived from the turbulence kinetic energy equation, is used to describe the streamwise development of the maximum Reynolds shear stress, $-\left(\overline{\rho u'v'}\right)_m$, or $\left(-\overline{u'v'}\right)_m$ for short, in conjunction with an assumed eddy-viscosity distribution which has $\sqrt{\left(-\overline{u'v'}\right)_m}$ as its velocity scale. In the outer part of the boundary-layer, the eddy viscosity is treated as a free parameter that is adjusted to satisfy the ODE for the maximum Reynolds shear stress. More specifically, the nonequilibrium eddy-viscosity distribution is defined again by separate expressions in the inner and outer regions of the boundary-layer. In the inner region, $(\varepsilon_m)_i$ is given by

$$(\varepsilon_m)_i = (\varepsilon_{mi})_1 (1 - \gamma_2) + (\varepsilon_{mi})_{J-K} \gamma_2 \qquad (15)$$

where $(\varepsilon_{mi})_1$ is given either by $(\kappa y)^2 \partial u/\partial y$ or $u_\tau y$. The expression $(\varepsilon_{mi})_{J-K}$ is

$$(\varepsilon_{mi})_{J-K} = D^2 \kappa y u_m \qquad (16)$$

where

$$u_m = max\left(u_\tau, \sqrt{\left(\overline{-u'v'}\right)_m}\right) \qquad (17a)$$

and D is a damping factor similar to that defined by Eq. (2a),

$$D = 1 - exp\left(\sqrt{\left(\overline{-u'v'}\right)_m} \frac{y}{\nu A^+}\right) \qquad (17b)$$

with the value of A^+ equal to 17 rather than 26, as in Eq. (2a). The parameter γ_2 in Eq. (15) is given by

$$\gamma_2 = tanh\left(\frac{y}{L_c'}\right) \qquad (17c)$$

where, with y_m corresponding to the y-location of maximum turbulent shear stress, $\left(-\overline{u'v'}\right)_m$,

$$L_c' = \frac{u_\tau}{u_\tau + u_m} L_m \qquad (18)$$

with

$$L_m = \begin{cases} 0.4 y_m & y_m \le 0.225\delta \\ 0.09\delta & y_m > 0.225\delta \end{cases} \qquad (19)$$

In the outer region, $(\varepsilon_m)_o$ is given by

$$\left(\varepsilon_m\right)_o = \sigma\left(0.0168 u_e \delta^* \gamma\right) \qquad (20)$$

where σ is a parameter to be determined. The term multiplying σ on the right-hand side of Eq. (20) is the same as the expression given by Eq. (5) without γ_{tr} and with $\alpha = 0.0168$.

The nonequilibrium eddy viscosity across the whole boundary-layer is computed from

$$\varepsilon_m = \left(\varepsilon_m\right)_o \tanh\left[\frac{\left(\varepsilon_m\right)_i}{\left(\varepsilon_m\right)_o}\right] \qquad (21)$$

The maximum Reynolds shear stress $\left(-\overline{u'v'}\right)_m$ is computed from the turbulence kinetic energy equation using assumptions similar to those used by Bradshaw et al.[10] After the modeling of the diffusion, production and dissipation terms and the use of

$$\frac{\left(-\overline{u'v'}\right)_m}{k_m} = a_1 = 0.25$$

the transport equation for $\left(-\overline{u'v'}\right)_m$ with u_m now denoting the streamwise velocity at y_m, is written as

$$\frac{d}{dx}\left(-\overline{u'v'}\right)_m = \frac{a_1\left(-\overline{u'v'}\right)_m}{L_m u_m}\left[\left(-\overline{u'v'}\right)_{m,eq}^{\frac{1}{2}} - \left(\overline{u'v'}\right)_m^{\frac{1}{2}}\right] - \frac{a_1}{u_m} D_m \qquad (22)$$

where, with $c_{dif} = 0.5$, the turbulent diffusion term along the path of maximum $\left(-\overline{u'v'}\right)$ is given by

$$D_m = \frac{c_{dif}}{a_1 \delta} \frac{\left(-\overline{u'v'}\right)_m^{\frac{3}{2}}}{\left[0.7 - (y/\delta)_m\right]} \left\{1 - \left[\frac{\left(-\overline{u'v'}\right)_m}{\left(-\overline{u'v'}\right)_{m,eq}}\right]^{\frac{1}{2}}\right\} \qquad (23)$$

To use this closure model, the continuity and momentum equations are first solved with an equilibrium eddy viscosity $(\varepsilon_m)_{eq}$ distribution such as in the CS model, and the maximum Reynolds shear stress distribution is determined based on $(\varepsilon_m)_{eq}$, which we denote by $\left(-\overline{u'v'}\right)_{m,eq}$. Next the location of the maximum Reynolds shear stress is determined so that y_m and u_m can be calculated. The transport equation for $\left(-\overline{u'v'}\right)_m$ is then solved to calculate the nonequilibrium eddy-viscosity distribution ε_m given by Eq. (21) for an assumed value of σ so that the solutions of the continuity and momentum equations can be obtained. The new maximum shear stress term is then compared with the one obtained from the solution of Eq. (22). If the new computed value does not agree with the one from Eq. (22), a new value of σ is used to compute the outer eddy viscosity and eddy-viscosity distributions across the whole boundary-layer so that a new $\left(-\overline{u'v'}\right)_m$ can be computed from the solution of the continuity and momentum equations. This iterative procedure of determining σ is repeated until $\left(-\overline{u'v'}\right)_m$ is computed from the continuity and momentum equations agrees with that computed from the transport equation, Eq. (22).

Another approach to improve the predictions of the CS model flows with adverse pressure gradient and separation is to relate the parameter α to a parameter F, according to the suggestion of Simpson, et al.,[11] by

$$\alpha = \frac{0.0168}{F^{1.5}} \qquad (24)$$

Here $(1 - F)$ denotes the ratio of the production of the turbulence energy by normal stresses to that by shear stress, evaluated at the location where shear stress is maximum, that is

$$F = 1 - \left[\frac{\left(\overline{u'^2} - \overline{v'^2}\right) \partial u/\partial x}{-\overline{u'v'}\, \partial u/\partial y}\right] \qquad (25)$$

Before (24) can be used in Eq. (5), an additional relationship between $\left(\overline{u'^2} - \overline{v'^2}\right)$ and $\left(-\overline{u'v'}\right)$ is needed. For this purpose, the ratio in Eq. (25)

$$\beta = \left[\frac{\overline{u'^2} - \overline{v'^2}}{-\overline{u'v'}} \right] \qquad (26)$$

is assumed to be a function of $R_t = \tau_w / \left(-\rho \overline{u'v'}\right)_m$ which, according to the data of Nakayama, [12] can be represented by

$$\beta = \frac{6}{1 + 2R_t(2 - R_t)} \qquad (27a)$$

for $R_t < 1.0$. For $R_t \geq 1.0$, β is taken to be

$$\beta = \frac{2R_t}{1 + R_t} \qquad (27b)$$

Introducing the above relationships into the definition of F and using Eq. (21) results in the following expression for α

$$\alpha = \frac{0.0168}{\left[1 - \beta(\partial u/\partial x)/(\partial u/\partial y)\right]^{1.5}} \qquad (28)$$

where β is given by Eq. (27).

Another improvement to the CS model can be made by replacing the intermittency parameter γ in Eq. (6) by another intermittency expression recommended by Fiedler and Head.[13] According to the experiments conducted by Fiedler and Head,[13] it was found that the pressure gradient has a marked effect on the distribution of intermittency defined as the ratio of time turbulent to total time at any point so that it measures the probability of finding turbulent flow at any instant at the point considered. Their experiments indicated that in the boundary-layer proceeding to separation, the intermittent zone decreases in width and moved further from the surface as shape factor H increases. The reverse trend is observed with decreasing H in a favorable pressure gradient.

In the improved CS model the intermittency expression of Fiedler and Head is written in the form

$$\gamma = \frac{1}{2}\left[1 - erf \frac{[y - Y]}{\sqrt{2}\,\sigma}\right] \qquad (29)$$

where Y and σ are general intermittency parameters with Y denoting value of y for which $\gamma = 0.5$ and σ, the standard deviation. The dimensionless intermittency parameters Y/δ^* and σ/δ^* expressed as functions of H are shown in Fig. 1.

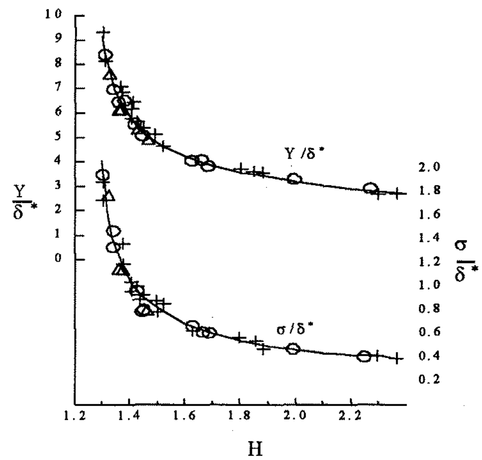

FIGURE 1 Variation of Y/δ^* and σ/δ^* with H according to the data of Fiedler and Head.

Results and Discussion

The predictions of the original and modified Cebeci-Smith turbulence models were investigated for several airfoils by using interactive boundary-layer and Navier-Stokes methods. For each airfoil, the onset of the transition location was computed with Michel's correlation[14] and the calculated lift coefficients were compared with data for a range of angles of attack, including stall and post stall.

Predictions of the Original and Improved CS Model by the Interactive Boundary-Layer Method of Cebeci[14]

A complete description and evaluation of the interactive boundary-layer (IBL) method used here is presented in Cebeci[14] for high and low Reynolds numbers at low Mach numbers and for a wide range of angles of attack. This method employs an inverse boundary-layer procedure in which the governing equations are solved for a compressible flow with the inviscid flow and viscous flow equations coupled with Veldman's interaction law. The inviscid flow is computed either with a panel method or a full potential method. In the former case, compressibility effects are introduced by using the Prandtl-Glauert correction.

Figures 2a to 2e show the results obtained with the original and modified CS models, the latter corresponding to the one in which α is computed according to Eq. (28) and the intermittency factor due to Fiedler and Head. The experimental data in Figures 2a to 2c were obtained by Carr et al.(15) and those in Figures 2d and 2e by Omar et al.(16) In all cases the inviscid flow calculations were made by using the full potential method.

As can be seen, the calculated results obtained with the modified CS model are significantly better than those obtained with the original CS model. In almost all cases, the calculated lift coefficients with the original CS model are much higher than those measured ones; in one case, Fig. 2d, the $(C_\ell)_{max}$ is not predicted at all. The modified CS model, on the other hand, in most cases, predicts the $(C_\ell)_{max}$ and produces lift coefficients for post stall which are in agreement with the trend of measured values.

Figures 3a to 3e show a comparison between the calculations and experimental results in which the calculated ones were obtained by using the modified CS and Johnson-King (JK) models. Overall, the predictions of the modified CS model are better than the JK model. For example, for the NACA 0012 airfoil, Fig. 3a, the modified CS model predicts $(C_\ell)_{max}$ more accurately than the JK model. For the Wortmann airfoil, Fig. 3b, the JK model does not predict the post-stall behavior of the lift coefficient. For the Ames airfoil, Fig. 3c, the predictions of both models are satisfactory with those obtained with the JK model are slightly better near $(C_\ell)_{max}$ than those with the CS model. For Boeing airfoils, the predictions of the modified CS model are better than the JK model near stall and especially post stall regions.

Predictions with a Navier-Stokes Method

The predictions of the original and modified CS models were also investigated by using the Navier-Stokes method of Swanson and Turkel.(6) The models considered include the original CS model, BL model, modifications to the BL model and the JK model.

Figures 4a to 4e show the results obtained with the original CS and BL models. In the former case, the length scale δ^* in the outer eddy-viscosity formula was computed based on the definition of the boundary-layer thickness δ given by Stock and Haase(3) and Johnson.(7)

Figures 5a to 5e show similar comparisons with turbulence models corresponding to the original CS and modified CS models. In the latter case the boundary-layer thickness was computed from

$$\delta = 1.5\, y_{1/2} \tag{30a}$$

or from

$$\delta = y_m \tag{30b}$$

if $1.5\, y_{1/2} > y_m$, with y_m corresponding to the location where streamwise velocity u is maximum. Figures 6a to 6e show results obtained with turbulence models based on modified CS and BL-JK models. In the latter case, the parameter α in the BL method was taken as a variable computed by the JK method.

A comparison of results presented in Figures 4 and 5 show that for the airfoil flows considered here, the results obtained with the original CS model (Fig. 4) with δ defined by Stock and Haase(3) and Johnson(7) are slightly better than those given by the BL model and the results with the modified CS model (Fig. 5) are much better than all the other modified versions of the original CS model.

A comparison of the results obtained with the modified CS model and with the BL-JK model (Fig. 6) show that both models essentially produce similar results.

Finally, Fig. 7 shows a comparison between the predictions of the IBL and NS methods. In both methods, the turbulence model used is the modified CS model. The IBL calculations made use of the full potential method discussed by Cebeci.(14) As can be seen, the predictions of both methods are identical at low and moderate angles of attack. At higher angles, especially near stall and post stall, while there are some differences, both methods predict the stall angle well. The savings in computing cost provided by the IBL method, however, is considerably less than those provided by the Navier-Stokes method.

References

1. Baldwin, B.S. and Lomax, H., "Thin Layer Approximation of Algebraic Model for Separated Turbulent Flows," AIAA paper No. 78-257, Jan. 1978.
2. Cebeci, T. and Smith, A.M.O., *Analysis of Turbulent Boundary-Layers,* Academic Press, NY, 1974.
3. Stock, H.W. and Haase, W., "Determination of Length Scales in Algebraic Turbulence Models for Navier-Stokes Methods," *AIAA J.,* Vol. 27, No.1, pp. 5-14, 1989.
4. Cebeci, T., Roknaldin, F. and Carr, L.W.,

"Prediction of Stall and Post-Stall Behavior of Airfoils at Low and high Reynolds Numbers," AIAA paper No. 93-3502, Jan. 1993.

5. Cebeci, T., Hefazi, H., Roknaldin, F. and Carr, L.W., "Prediction of Compressibility Effect on Airfoil Stall at Low Mach Numbers," AIAA paper No. 94-0290, Jan. 1994.
6. Swanson, R.C., Turkel, E., "A Multistage Time-Stepping Scheme for the Navier-Stokes Equations," AIAA paper No. 85-0035, Jan. 1985.
7. Johnson, D.A., "Nonequilibrium Algebraic Turbulence Modeling Considerations for Transonic Airfoils and Wings," AIAA paper No. 92-0026, Jan. 1992.
8. Johnson, D.A. and King, L.S., "Mathematically Simple Turbulence Closure Model for Attached and Separated Turbulent Boundary Layers," *AIAA J,* Vol. 23, No. 11, pp. 1684-1692, 1985.
9. Johnson, D.A. and Coakley, T.J., "Improvement to a Nonequilibrium Algebraic Turbulence Model," *AIAA J,* Vol. 28, No. 11, pp. 2000-2003, 1990.
10. Bradshaw, P., Ferriss, D.H. and Atwell, N.P., "Calculation of Boundary-Layer Development Using the Turbulent Energy Equation," *J. Fluid Mech.,* Vol. 18, p. 593, 1967.
11. Simpson, R.L., Chew, Y.T. and Shivaprasad, B.G., "The Structure of a Separating Turbulent Boundary Layer, Part 1, Mean Flow and Reynolds Stresses," *J. Fluid Mech.,* Vol. 113, pp. 23-51, 1981.
12. Nakayama, A., "Measurements in the Boundary Layer and Wake of Two Airfoil Models," Report No. MDC J2403, Douglas Aircraft Co., June 1982.
13. Fiedler, H. and Head, M.R., "Intermittency Measurements in the Turbulent Boundary Layer," *J. Fluid Mech.,* Vol. 25, Part 4, pp. 719-735, 1966.
14. Cebeci, T., *An Engineering Approach to the Calculation of Aerodynamic Flows,* to be published, 1996.
15. Carr, L.W., McCroskey, W.J., McAlister, K.W., Pucci, S.L. and Lambert, O., *An Experimental Study of Dynamic Stall on Advanced Airfoil Sections, Vol. 3, Hot-Wire and Hot-Film Measurements,* NASA TM 84245.
16. Omar, E., Zierten, T., Hahn, M., Szpiro, E. and Mahal, A., *Two-Dimensional Wind-Tunnel Tests of a NASA Supercritical Airfoil with Various High-Lift Systems, Vol. 2, Test Data,* NASA CR-2215, 1977.

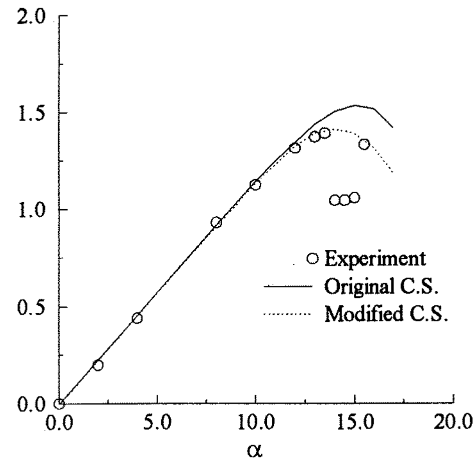

(a)

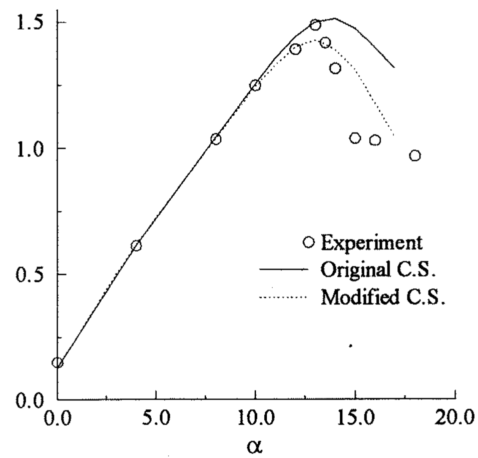

(b)

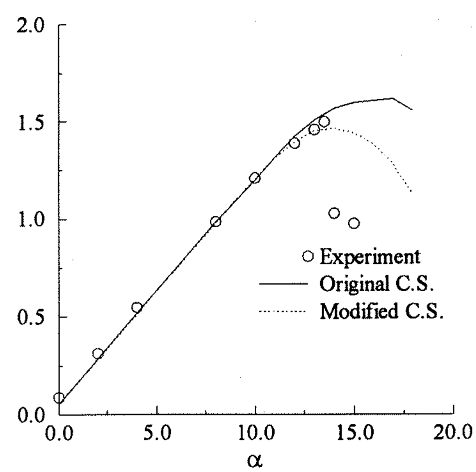

(c)

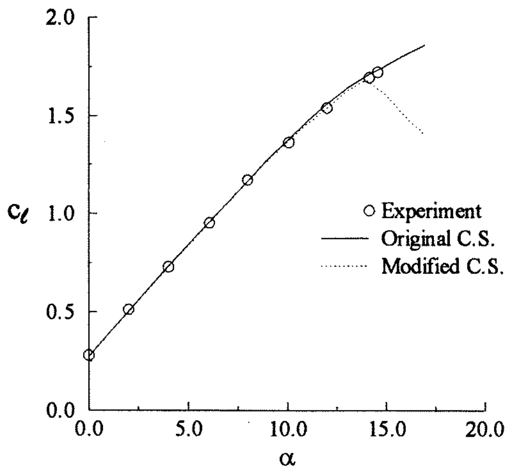

(d)

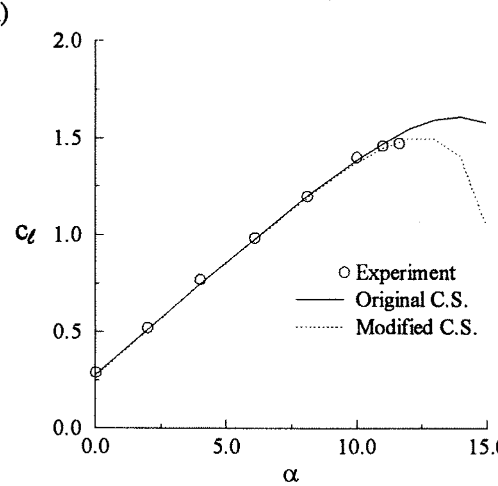

(e)

FIGURE 2 IBL results for the (a) NACA 0012 airfoil; (b) Wortmann airfoil; (c) Ames airfoil; (d) Boeing airfoil, $M_\infty = 0.2$; and (e) Boeing airfoil, $M_\infty = 0.3$.

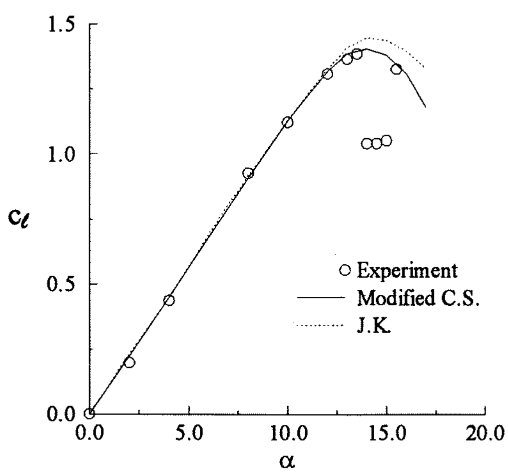

(a)

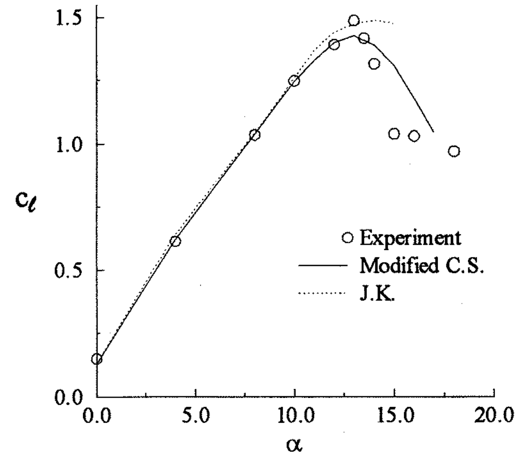

(b)

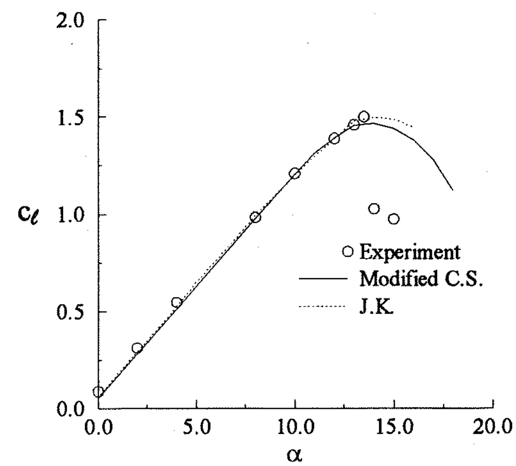

(c)

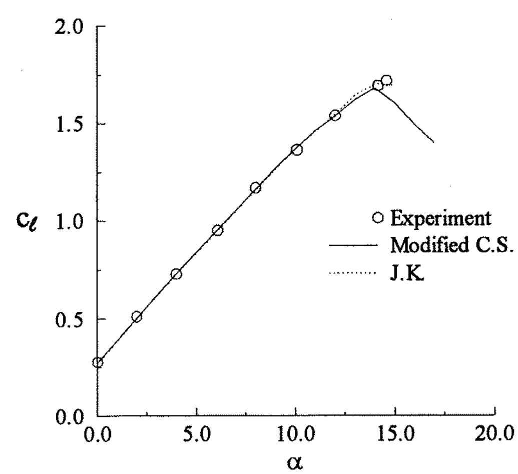

(d)

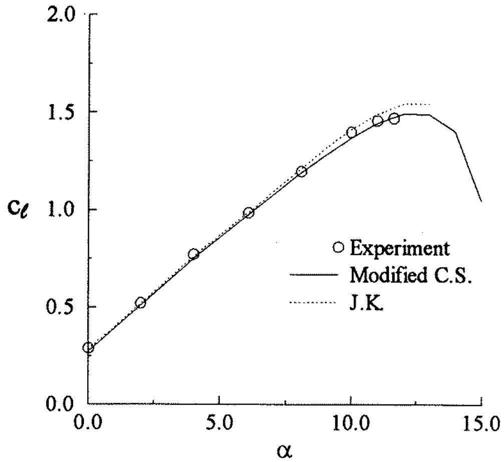

(e)

FIGURE 3 IBL results for the (a) NACA 0012 airfoil; (b) Wortmann airfoil; (c) Ames airfoil; (d) Boeing airfoil, $M_\infty = 0.2$; and (e) Boeing airfoil, $M_\infty = 0.3$.

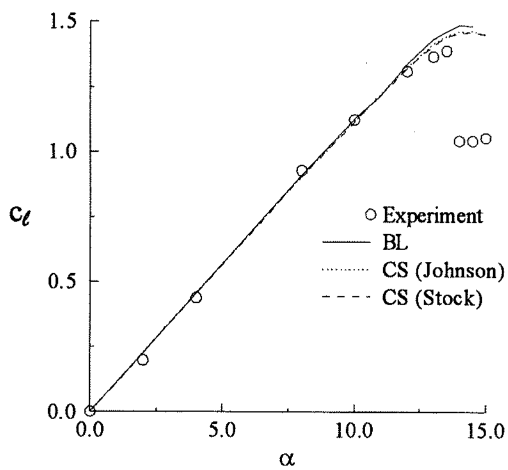

(a)

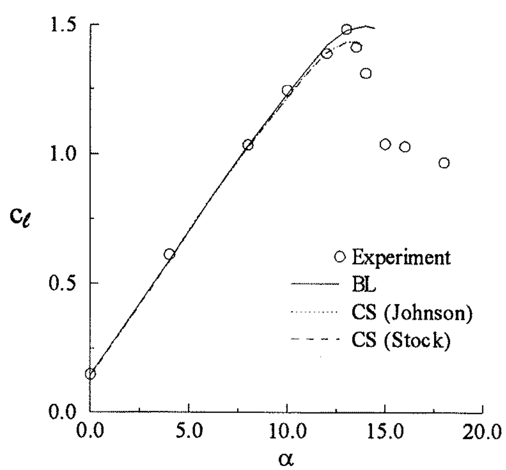

(b)

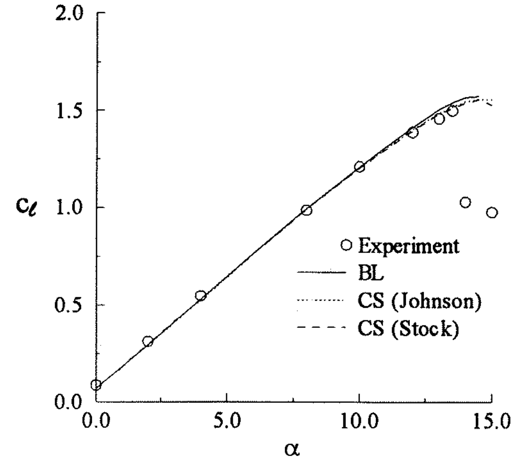

(c)

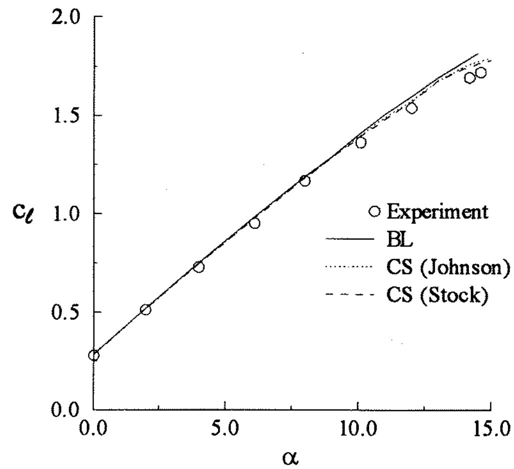

(d)

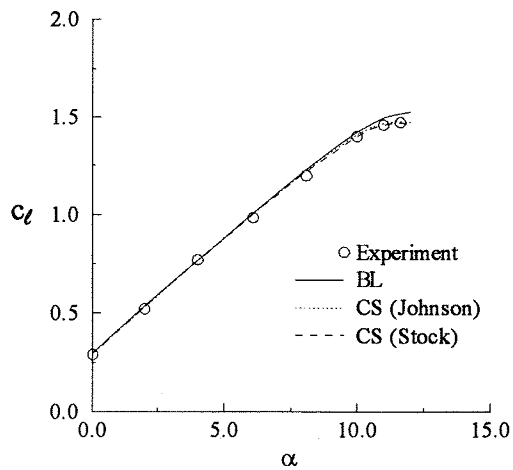

(e)

FIGURE 4 NS results for the (a) NACA 0012 airfoil; (b) Wortmann airfoil; (c) Ames airfoil; (d) Boeing airfoil, $M_\infty = 0.2$; and (e) Boeing airfoil, $M_\infty = 0.3$.

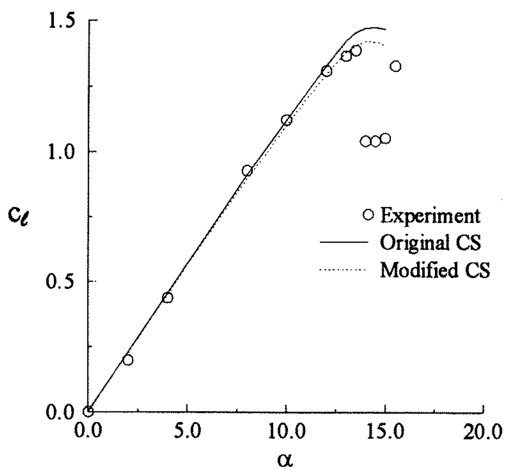

(a)

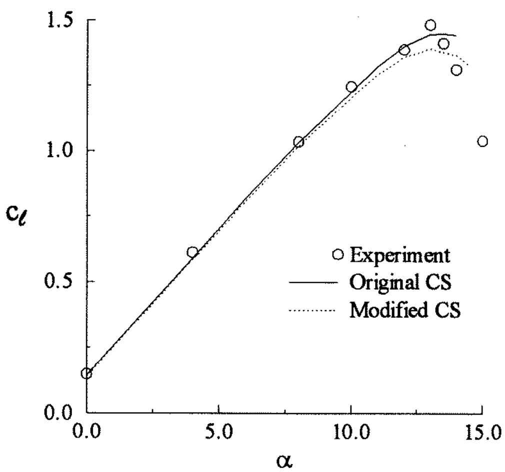

(b)

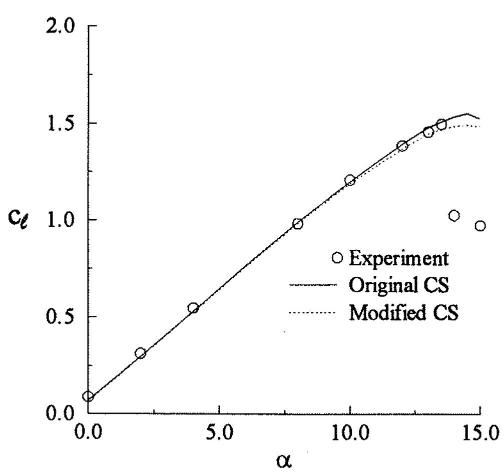

(c)

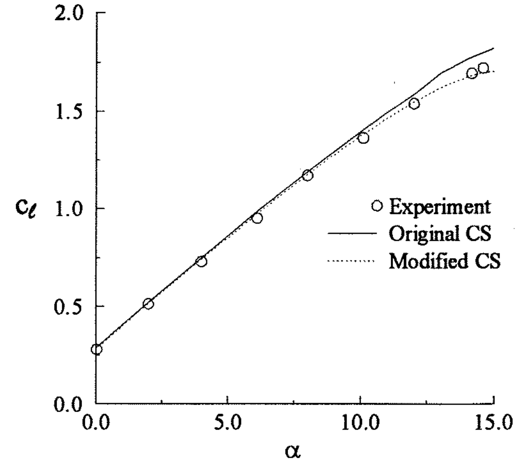

(d)

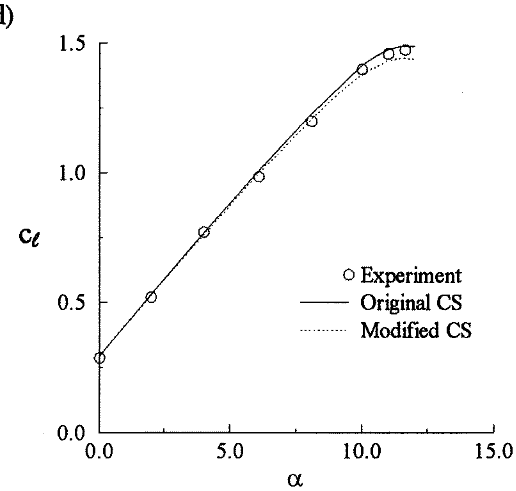

(e)

FIGURE 5 NS results for the (a) NACA 0012 airfoil; (b) Wortmann airfoil; (c) Ames airfoil; (d) Boeing airfoil, $M_\infty = 0.2$; and (e) Boeing airfoil, $M_\infty = 0.3$.

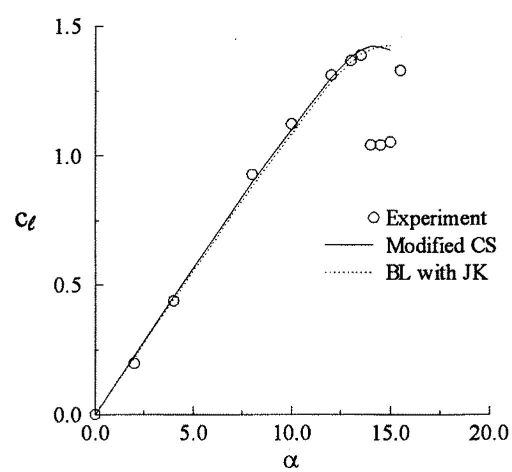

(a)

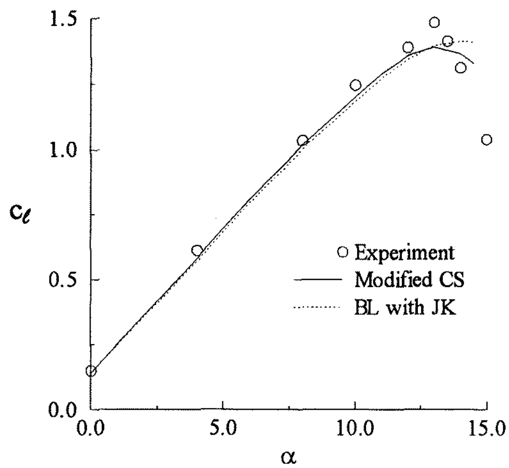

(b)

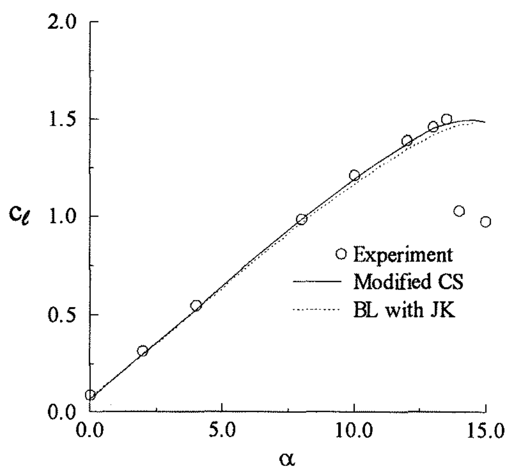

(c)

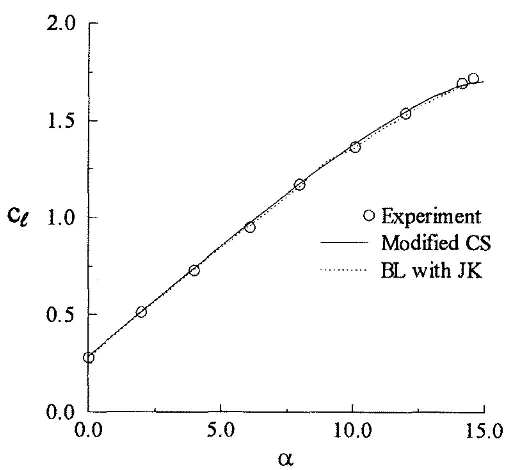

(d)

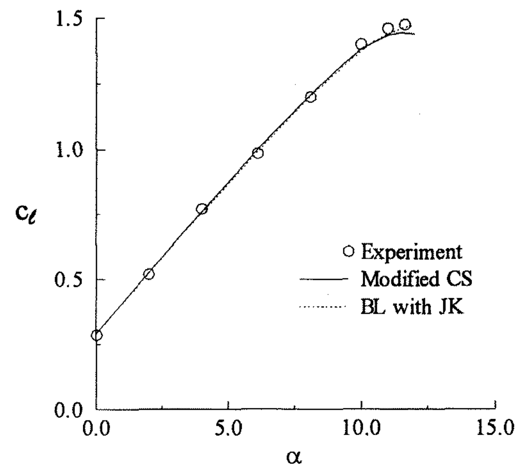

(e)

FIGURE 6 NS results for the (a) NACA 0012 airfoil; (b) Wortmann airfoil; (c) Ames airfoil; (d) Boeing airfoil, $M_\infty = 0.2$; and (e) Boeing airfoil, $M_\infty = 0.3$.

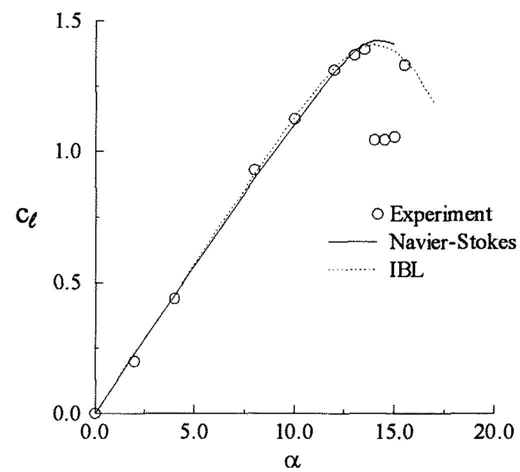

(a)

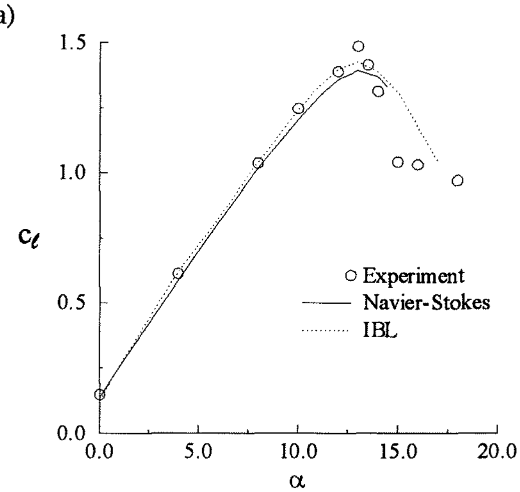

(b)

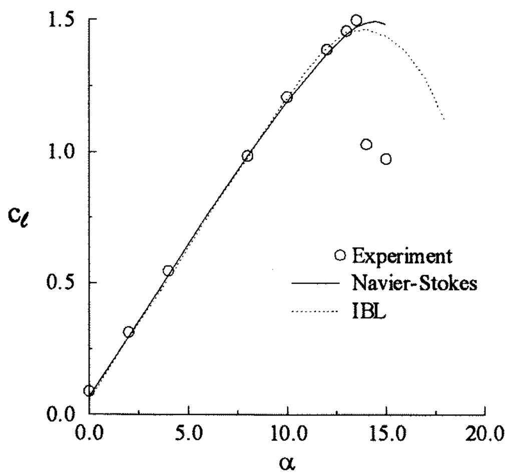

(c)

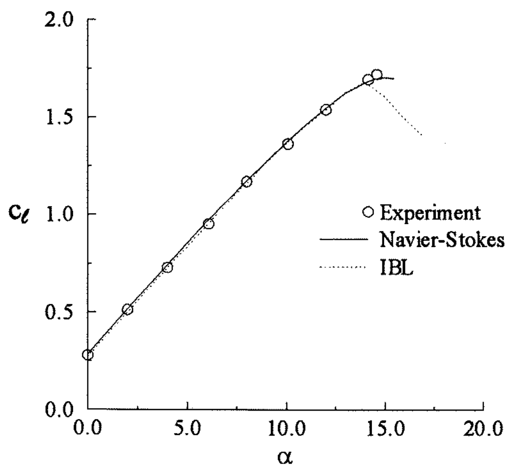

(d)

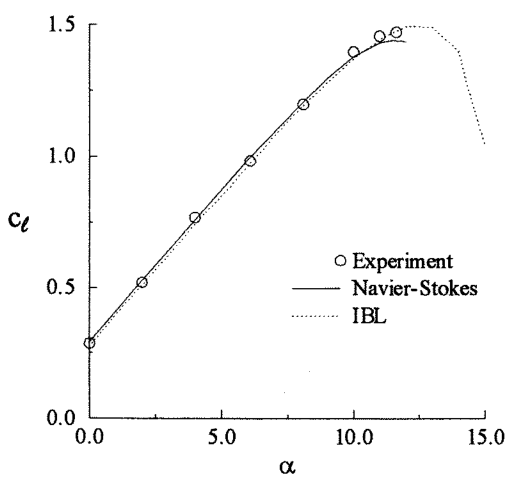

(e)

FIGURE 7 Comparison of NS and IBL results obtained with the modified CS model for the (a) NACA 0012 airfoil; (b) Wortmann airfoil; (c) Ames airfoil; (d) Boeing airfoil, $M_\infty = 0.2$; and (e) Boeing airfoil, $M_\infty = 0.3$.